water

MDPI

Article

Ctenopharyngodon idella's Movement Behavior in Response to Hydraulics at Fishway Entrance with Different Entrance Angles

Yiming Mi [1,2], Junjun Tan [1,2,*], Honglin Tan [1,2], Junjian Sun [1,2], Senfan Ke [1,2], Minne Li [1,2], Chenyu Lin [1,2] and Xiaotao Shi [1,2,*]

[1] Hubei International Science and Technology Cooperation Base of Fish Passage, China Three Gorges University, Yichang 443002, China; yudaomiyiming@126.com (Y.M.); thl1642709374@126.com (H.T.); sun_jj1@163.com (J.S.); ksfctgu@163.com (S.K.); liminne@ctgu.edu.cn (M.L.); linchenyu@ctgu.edu.cn (C.L.)
[2] College of Hydraulic and Environmental Engineering, China Three Gorges University, Yichang 443002, China
* Correspondence: tanjunjun52@163.com (J.T.); fishlab@163.com (X.S.)

Abstract: The hydrodynamics at the fishway entrance play an important role in attracting fish into a fishway. Adjusting the entrance angle of the fishway to allow suitable water flow patterns at the entrance is an effective measure that can be used to improve the attraction efficiency. In this study, we analyzed the movement behavior of grass carp (*Ctenopharyngodon idella*) in a river channel at a fishway entrance with different fishway entrance angles (30°, 45°, and 60°) and different replenishment velocities (0.1 m/s, 0.2 m/s, and 0.3 m/s). The flow velocity was 0.32–0.50 m/s when the fish head deflected into the entrance under different entrance angles for grass carp. As the entrance angle of the fishway increased, the fish energy consumption increased. The range of energy consumption for grass carp increased from 1.26–3.59 × 10^{-3} J to 3.32–7.33 × 10^{-3} J when the entrance angle was increased from 30° to 60°. There was a negative correlation between the entrance angle of the fishway and the deflection angle of the tested fish's head. This research presents a reference that combines fish swimming behavior and hydraulics to optimize the design of fishway entrances.

Keywords: fishway entrance; entrance angle; fish movement behavior; energy consumption; grass carp

check for updates

Citation: Mi, Y.; Tan, J.; Tan, H.; Sun, J.; Ke, S.; Li, M.; Lin, C.; Shi, X. *Ctenopharyngodon idella*'s Movement Behavior in Response to Hydraulics at Fishway Entrance with Different Entrance Angles. *Water* **2024**, *16*, 2168. https://doi.org/10.3390/w16152168

Received: 21 June 2024
Revised: 27 July 2024
Accepted: 29 July 2024
Published: 31 July 2024

1. Introduction

The construction of hydraulic structures such as dams, sluice gates, and weirs has blocked the connectivity of rivers and fragmented migration routes [1–6]. Fishways were developed to restore river connectivity and provide a passage for migrated fish species [7,8]. However, the dimensions of fishway entrances are small compared to those of rivers, and the hydrodynamic change of rivers affects the velocities at fishway entrances and the attraction of fish to these entrances [1]. Therefore, the design of the entrance is important for attracting fish into a fishway [9,10].

Currently, studies on fishway entrances have mainly focused on the location and arrangement of these entrances and their water replenishment. For instance, a suitable location for a fishway entrance is the fish aggregation zone downstream of a dam [10]. When the fishway entrance is arranged near the dam, the conditions are more attractive to the target fish [11,12]. A certain angle between the direction of the fishway entrance and the main flow direction of the river can attract fish to cross into the fishway entrance [13]. If the flow directions from the fishway and the replenishment discharge differ, their merging enhances the ambivalent signals, affecting fish movement orientation [14]. Thus, suitable fishway entrance angles and replenishment flow would be beneficial to attract fish into the entrance. To understand how a fishway entrance and its replenishment water flow attract fish under variable flow, it is important to identify how the hydraulic factors affect fish movement behaviors [15,16]. Suitable water flow conditions are the key to the attraction and entrance efficiency of fishways [17,18]. The main hydraulic factor that affects the attraction and entrance efficiency of a fishway is water velocity. When the velocity at the entrance is higher than the burst swimming speed or lower than the induced flow speed of fish species, the water flow at the entrance is not enough to make the fishway attractive [19–21]. Energy consumption is an important indicator used to present the relationship between fish behavior and hydraulic factors [22]. When fish move in a river or channel, they must use energy to resist the water flow [23,24]. Studies have found that fish consume more energy in response to excessive turbulent kinetic energy [20,25–27]. For example, juvenile rainbow trout (*Oncorhynchus mykiss*) preferred positions with low turbulence and high flow velocity at low discharge but low flow velocity and high turbulence at high discharge [28]. Grass carp avoided the zone where the turbulent kinetic energy was greater than 0.012 m^2/s^2 in the upstream movement route [29], and bighead carp required more energy in high-TKE zones [26]. Thus, energy consumption was analyzed in relation to varied entrance angles and replenishment water flows.

Grass carp (*Ctenopharyngodon idella*) is an economic fish species in the Yangtze River and is recognized as the most important freshwater fish species in China [30–32]. This species has a migratory requirement between rivers and lakes [33]. However, the abundance of this carp was reduced to just 4.2% of the average in 2005 [34]. It is urgent to provide an effective fishway entrance and replenishment discharges to attract fish into the fishway. Thus, this study aimed to analyze the swimming behavior of grass carp in response to different entrance angles and replenishment flows. Specifically, the primary objectives of this study were to (a) analyze the effects of different entrance angles and replenishment discharges on the attraction efficiency of fishways and (b) understand the swimming behavior in response to different entrance angles and replenishment discharges.

2. Materials and Methods

2.1. Experiment Fishway

A 1:10 physical model was installed at China Three Gorges University, China. The model structure was constructed of concrete with dimensions of 7.02 m (length) × 2.46 m (width) × 0.50 m (height), which included an entrance to the fishway and a water replenishment channel (Figure 1). The "*x*" direction is parallel to the flow, and the "*y*" direction is perpendicular to it. The entire experimental zone included the test zone (5.20 m × 2.46 m × 0.50 m) and acclimation zone (1.82 m × 2.46 m × 0.50 m). Moreover, the water depth in the channel was controlled using a tailgate, and the flow in the replenishment channel was provided by a gauging weir. Three fishway entrances with different entrance angles (30°, 45°, and 60°) were studied, labeled as types 1, 2, and 3, respectively. A concrete head tank (2.0 m length × 1.5 m height × 1.2 m width) located upstream of the fishway supplied water flow into the channel.

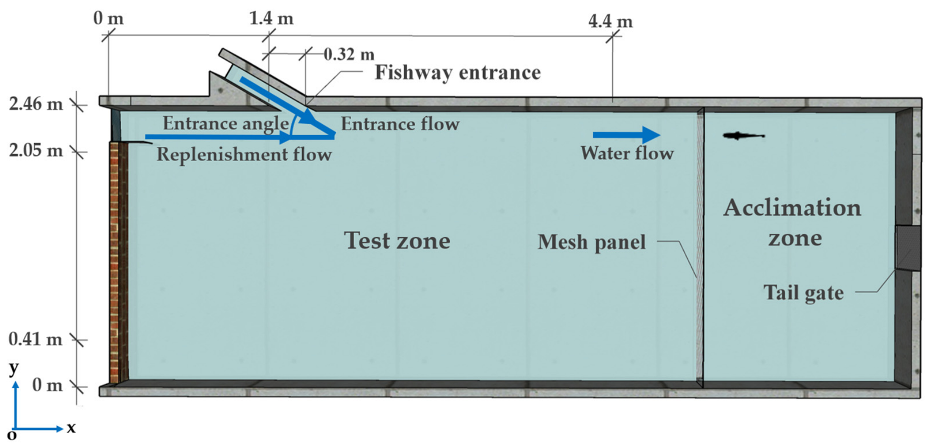

Figure 1. Schematic of the experimental river channel including the replenishment channel and different entrance angle (30°, 45°, and 60°) to test fish species grass carp.

Three types of fishway entrance with different entrance angles (30°, 45°, and 60°) and different velocities of replenishment flow (0.1 m/s, 0.2 m/s, and 0.3 m/s) were used for the experiment. The fishway entrance angle is defined as the angle of the inclined entrance. The entrance flow velocity was adjusted to 0.4 m/s based on the swimming capability of grass carp [31–33,35]. The velocity of replenishment flow was sequentially adjusted to three design conditions (0.1 m/s, 0.2 m/s, and 0.3 m/s). A total of 187 experimental fish were used in the study and assigned to different angles and flow conditions (Table 1).

Table 1. The details of the experimental conditions testing fish movement behavior in nine working conditions regarding different entrance angles and replenished flow.

Fish Species	Entrance Angles	Working Conditions	Velocity of Replenishment Channel/(m/s)	Number of Tested Fish (*N*)	Total Length /(cm)
Grass carp	30°	30–1	0.1	22	11.75 ± 1.00
		30–2	0.2	21	12.30 ± 1.74
		30–3	0.3	21	11.40 ± 2.40
	45°	45–1	0.1	22	12.50 ± 1.66
		45–2	0.2	20	13.16 ± 1.82
		45–3	0.3	21	13.39 ± 1.25
	60°	60–1	0.1	20	14.01 ± 2.24
		60–2	0.2	20	15.16 ± 1.25
		60–3	0.3	20	13.31 ± 0.92

Notes: 30–1, 30–2, and 30–3 represent each replenishment channel velocity (0.1 m/s, 0.2 m/s, and 0.3 m/s) for 30° fishway entrance tests. Similarly, 45–1, 45–2, and 4–3 represent each replenishment channel velocity (0.1 m/s, 0.2 m/s, and 0.3 m/s) for 45° fishway entrance tests, and 60–1, 60–2, and 60–3 represent each of the replenishment channel velocity (0.1 m/s, 0.2 m/s, 0.3 m/s) for 60° fishway entrance tests.

2.2. Hydraulics

Experimental conditions in the channel were shown in Table 1. Three fishway entrance angle (30°, 45°, and 60°) and three replenishment flow velocity (0.1 m/s, 0.2 m/s, and 0.3 m/s) were performed in our experiment. The water velocity of the entire channel was measured with a 16-MHz acoustic Doppler velocimeter (ADV; Son Tek Micro ADV, Son Tek, CA, USA). The probe was positioned in the flow with an adjustable traverse and caused negligible disturbance to the observed flow.

Velocity measurements were taken under the working condition of a fishway entrance angle of 45°, a fishway entrance velocity of 0.4 m/s, and a replenishment channel velocity of 0.2 m/s. Flow velocities were measured at a total of 20 points. Velocity measurements were taken at one horizontal plane (z = 0.09 m), which is parallel to the channel bottom. In addition, WinADV software (version 2.024) was used to obtain the data [36]. In order to obtain the hydraulics distribution in the whole test zone, the data obtained by ADV were used to validate the accuracy of the numerical simulation results.

2.3. Numerical Model

Computational fluid dynamics (CFD) software (Fluent 6.3, ANSYS Corporation, Canonsburg, PA, USA) with an RNG k–ε turbulence model was utilized to obtain the distribution of the flow field in the fishway. A velocity-type inlet boundary condition was adopted at the inlet of the fishway with the measured velocity value in the experiment. A pressure-type outlet boundary condition was given at the exit of the fishway. The model was discretized via the finite volume method using a hexahedron computing grid with 666,988 cells. Model validation was conducted with an entrance flow velocity of 0.4 m/s, velocity of the replenishment channel of 0.2 m/s, and a fishway entrance angle of 45°.

In order to validate the accuracy and reliability of the numerical simulations, the 10 measured points on sections x = 1.5 m and y = 1.96 to 2.46 m and the 10 measured points on sections x = 1.6 m and y = 1.96 to 2.46 m at z = 0.09 m (z denotes the water depth of the channel) were used to verify the model. The grid-independent analytical solution was validated at x = 1.5 m and y = 1.96 to 2.46 m. The three meshes had little influence on the calculation results, as shown in Figure 2. In order to ensure the accuracy of the numerical model, a mesh convergence analysis of the model was carried out (Table 2). Three hexahedral meshes with different numbers of computational meshes were tested; namely, mesh 1, mesh 2, and mesh 3. The number of cells for the three meshes was 520,542, 666,988, and 819,560, respectively. Figure 2 shows that the results of mesh 1, mesh 2, and mesh 3 were close to the measured values. Considering the calculation accuracy and efficiency, the mesh of 666,988 was selected as the calculation mesh. The simulated velocity values were compared with the corresponding experimentally measured values in the channel, as shown in Figure 3. The relative error between the simulated and measured values ranged from 3.22% to 19.83%, with an average relative error of 10.93%. In addition, there was a significant correlation between the measured and simulated velocity values (R_{1V}^2 = 0.985, R_{2V}^2 = 0.944) (Figure 4).

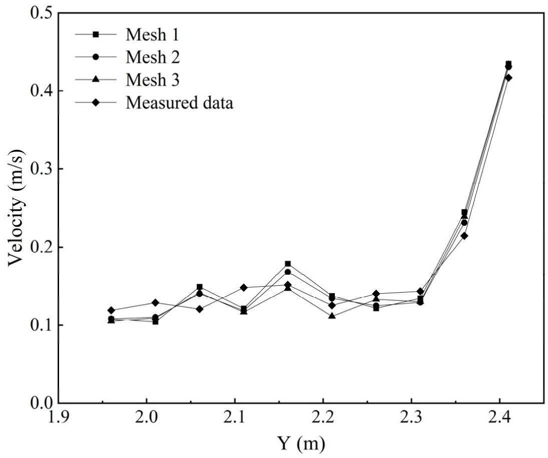

Figure 2. The results of the mesh convergence analysis on sections x = 1.6 m and y = 1.96–2.46 m (z = 0.09 m).

Table 2. The mesh convergence analysis of the model was carried out considering three meshes (mesh 1, mesh 2, and mesh 3).

Mesh	Cell Size	Number of Cells	Mesh
1	0.03–0.04 m	520,542	Coarse
2	0.03 m	666,988	Medium
3	0.02 m	819,560	Fine

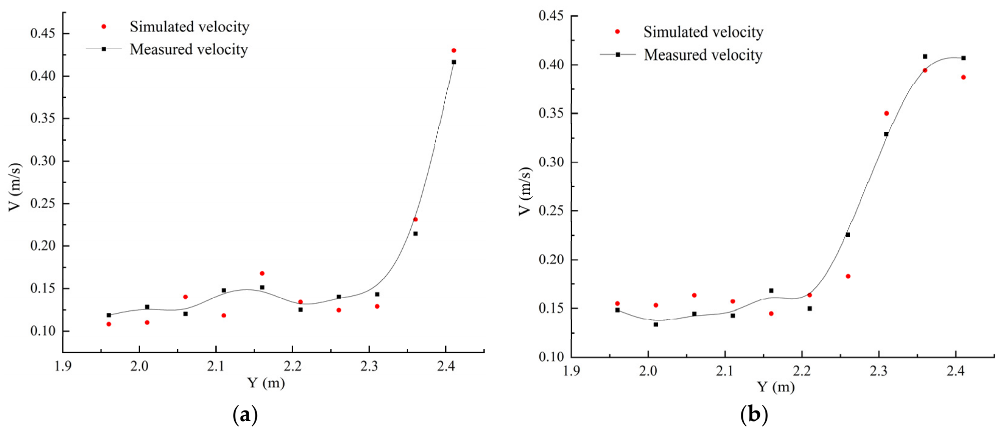

Figure 3. Comparison between the numerical simulated velocity and measured velocity: (**a**) P_1: y direction with x = 1.5 m (z = 0.09 m), (**b**) P_2: y direction with x = 1.6 m (z = 0.09 m).

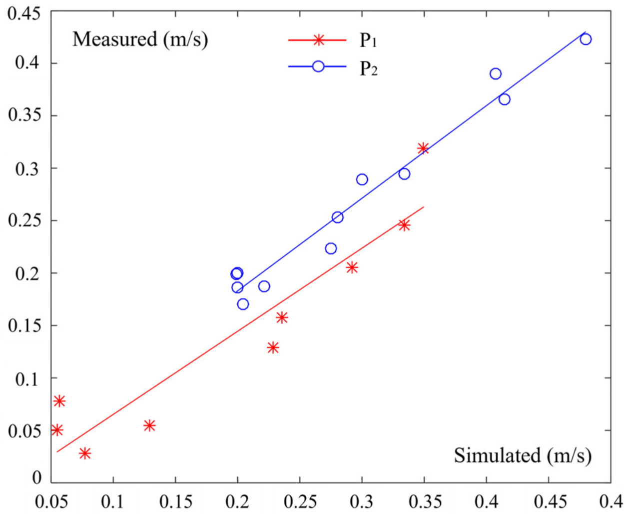

Figure 4. The simulated V values were compared with the corresponding measured values, as shown in Figure 2. Linear regression [37,38] of the simulated and measured V values in two different positions (P_1: y direction with x = 1.5 m (z = 0.09 m); P_2: y direction with x = 1.6 m (z = 0.09 m) is shown in Figure 3. ${R_{1V}}^2$ and ${R_{2V}}^2$ were 0.985 and 0.944, respectively.

2.4. Experimental Fish

Grass carp (N = 187) with a total length (TL) of 13.1 ± 1.7 cm (mean ± SD) were obtained from Qingjiang River, Hubei, China, and transported to China Three Gorges University via oxygenated plastic bags. All the fish were placed in an aerated acclimation tank with dimensions of 3.0 m (diameter) × 1.5 m (height) for 48 h prior to the beginning of the experiments. The mean water temperature was controlled at 21 °C and the dissolved oxygen level was 7.0 mg/L. The fish were kept in the tank for at least 5 days to recover from transport and handling stress. Additionally, the fish were fed on pond sticks (Tetra Gmbh) until 24 h prior to experimentation. Before the test, one fish was randomly selected and introduced to the acclimation zone for 20 min, and then the fish were allowed to volitionally move within 1 h after removing the mesh panel in the acclimation zone. According to the pre-test, if the fish did not enter the fishway entrance within 1 h, the test was ended.

A video monitoring system, including a 25-fps video camera (HIKVISION, Hangzhou, China), a computer, and data storage, was positioned 4 m above the channel to monitor the fish movements. Thus, fish behavior was continuously monitored using the video monitoring system. Logger Pro software (version 3.16.2) (Vernier Software & Technology, Beaverton, OR, USA) was used to determine the fish's movement behavior, and the swimming speed, migration transit time, transit position, and the number of fish attracted to the fishway entrance were obtained using the video.

2.5. Fish Movement Energetics

Energy consumption is an important factor used to explain fish's movement variation. The definition of the energy consumption (E) of fish is as follows:

$$E = \int_0^S |f| ds \tag{1}$$

where s is the fish's movement distances and f is the dragging force of the fish in the process of moving.

f is calculated as follows [39,40]:

$$f = 0.5 C_d \rho A_s \left(U_w - U_f \right)^2 \tag{2}$$

$$A_s = \alpha {L_f}^{\beta} \tag{3}$$

where ρ is the density of water, A_s is the wetted surface zone of fish, α = 0.465, and β = 2.11. C_d is the coefficient of drag, including the frictional drag coefficient C_f and the pressure drag coefficient C_p, considering that C_f is larger than C_d.

C_d is expressed using the following formula:

$$C_d = C_f + C_p \approx 1.2C_f \tag{4}$$

$$C_d = 0.074R_e^{-0.2} \tag{5}$$

$$R_e = \frac{U_f \times L_f}{v} \tag{6}$$

where R_e represents the Reynold's number of fish [41], and ν is the dynamic viscosity of water.

2.6. Data Analysis

The movement trajectories, position, transit time, and deflection angle of the tested fish's head were extracted from the monitoring video using tracker software. The fish deflection angle is defined as the angle of the fish head inclined to the main flow. The attraction efficiency, cumulative entrance efficiency, and deflection efficiency were calculated based on the monitored data. A one-way ANOVA test was used to test the difference in efficiency values among different entrance angles, performed using SPSS 22.0, with a threshold of 0.05.

The number of tested fish attracted to the fishway entrance and the number of fish that successfully entered the fishway were monitored to reflect the effectiveness of the fishway.

The attraction efficiency of a fishway (E_0) is defined as

$$E_0 = \frac{N_1}{N_0} \times 100\% \tag{7}$$

where E_0 is the attraction efficiency, N_1 is the number of fish that successfully reach the fishway entrance zone, and N_0 is the number of fish released for each design condition.

The cumulative entrance efficiency (E_1) is defined as

$$E_1 = \frac{N_2}{N_1} \times 100\% \tag{8}$$

where E_1 is the cumulative entrance efficiency, N_2 is the number of fish that successfully entered the fishway, and N_1 is the number of tested fish.

The deflection efficiency (E_2) is defined as

$$E_2 = \frac{N_4}{N_3} \times 100\% \tag{9}$$

where E_2 is the deflection efficiency, N_4 is the frequency of fish that successfully entered the fishway entrance after deflection, and N_3 is the total frequency of tested fish deflected in each work condition.

3. Results

3.1. Hydraulics

The water direction at the entrance of the channel changed with different entrance angles (Figure 5). The mainstream was gradually spread on the right bank with an increase in the entrance angle. The mainstream in the fishway entrance was mainly spread along the left bank at a 30° entrance angle, while two large recirculation zones appeared on each side of the mainstream at 45° and 60° entrance angles.

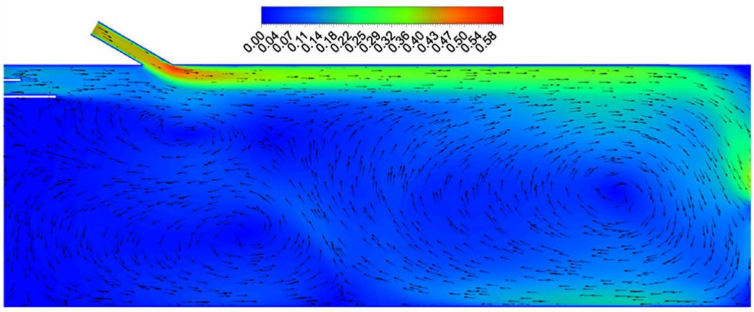

(30–1)

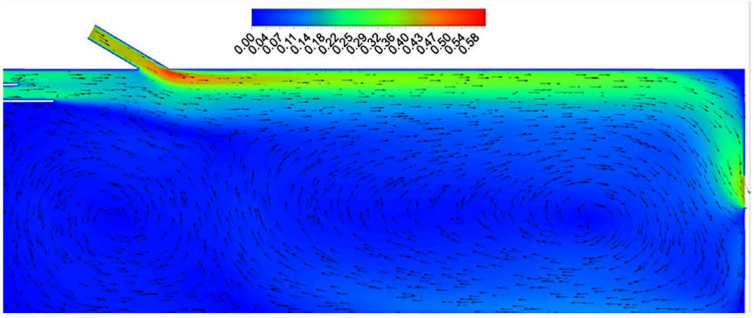

(30–2)

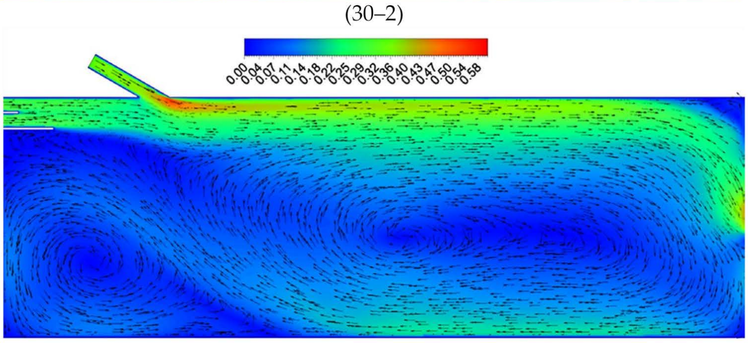

(30–3)

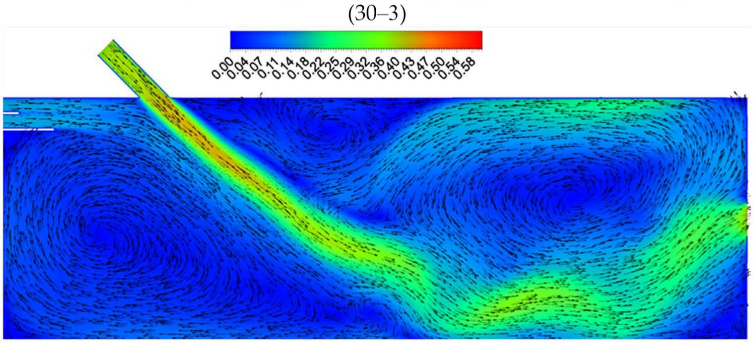

(45–1)

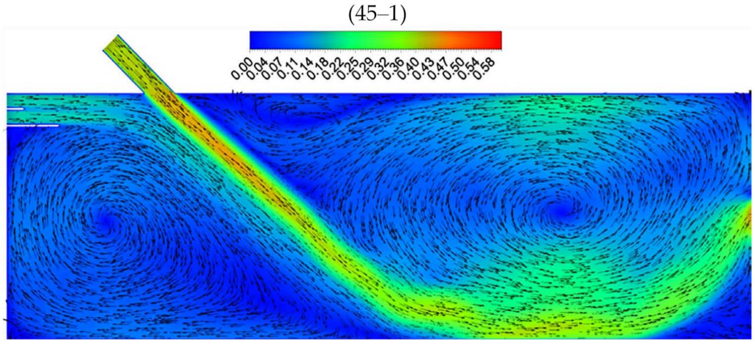

(45–2)

Figure 5. *Cont*.

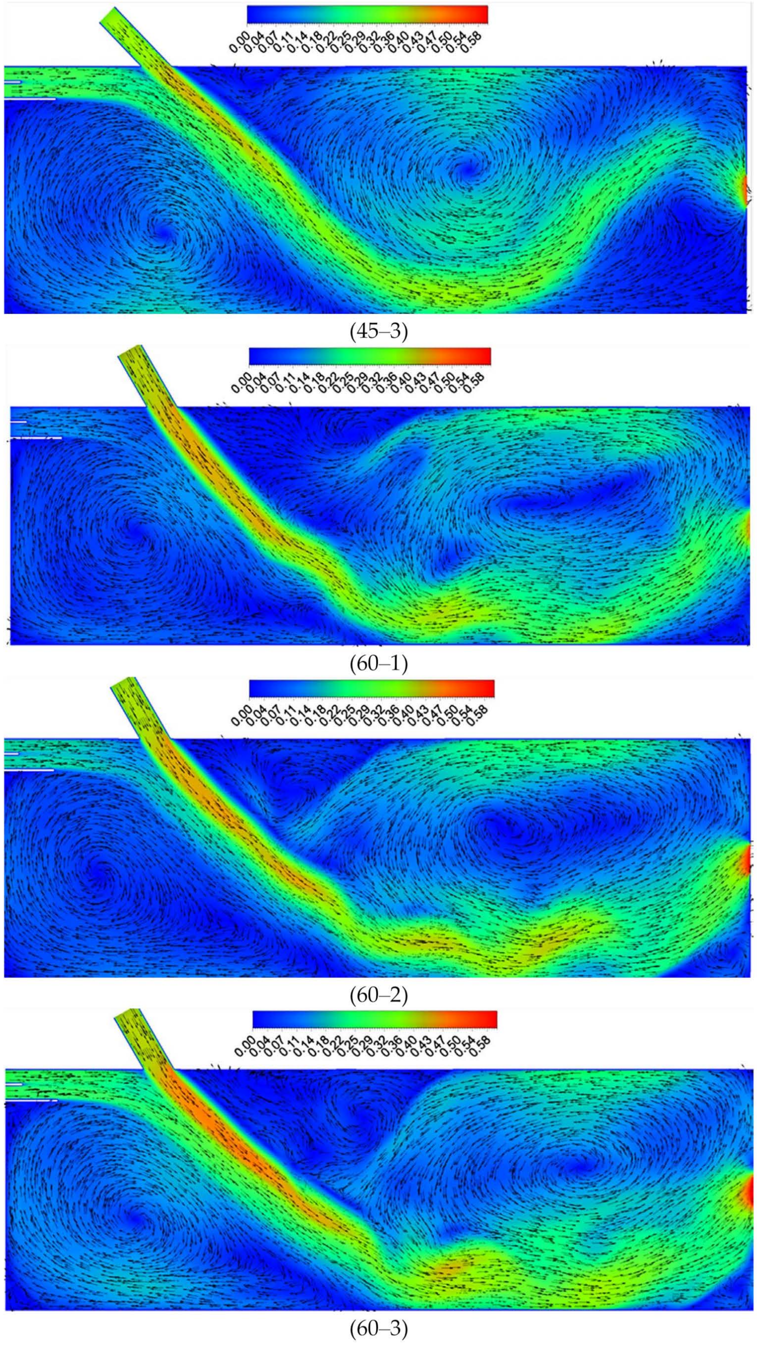

Figure 5. The velocity distribution of the experimental channel (note: 30–1, 30–2, 30–3, 45–1, 45–2, 45–3, 60–1, 60–2, and 60–3 represent the working conditions in Table 1).

At a 30° entrance angle, the maximum flow velocities near the entrance of the fishway could reach 0.514 m/s, 0.528 m/s, and 0.543 m/s when the velocity of the replenishment channel was 0.1 m/s, 0.2 m/s, and 0.3 m/s, respectively (Figure 5). When the entrance angle was 45°, the velocities near the fishway entrance ranged from 0.359 to 0.453 m/s, and the velocities near the fishway entrance ranged from 0.358 to 0.492 m/s at a 60° inlet entrance angle.

3.2. Fish Movement

When the entrance angle was 30° and the velocity of the replenishment channel was 0.1 m/s, 0.2 m/s, and 0.3 m/s, the cumulative entrance efficiency of grass carp was 50%, 45%, and 40%, respectively, and the transit time for entering the fishway was 2389 s, 2351 s, and 1517 s, respectively. When the entrance angle was 45° and the velocity of the replenishing channel was 0.1 m/s, 0.2 m/s, and 0.3 m/s, the cumulative entrance efficiency was 41%, 75%, and 81%, respectively, and the transit time for entering the fishway was 2156 s, 2146 s, and 1825 s for grass carp, respectively. Similarly, the cumulative entrance efficiency was 50%, 45%, and 40% for grass carp. At the same time, the transit time for entering the fishway was 2389 s, 2351 s, and 1517 s for grass carp at an entrance angle of 60° when the velocity of the replenishment channel was 0.1 m/s, 0.2 m/s, and 0.3 m/s, respectively (Figure 6).

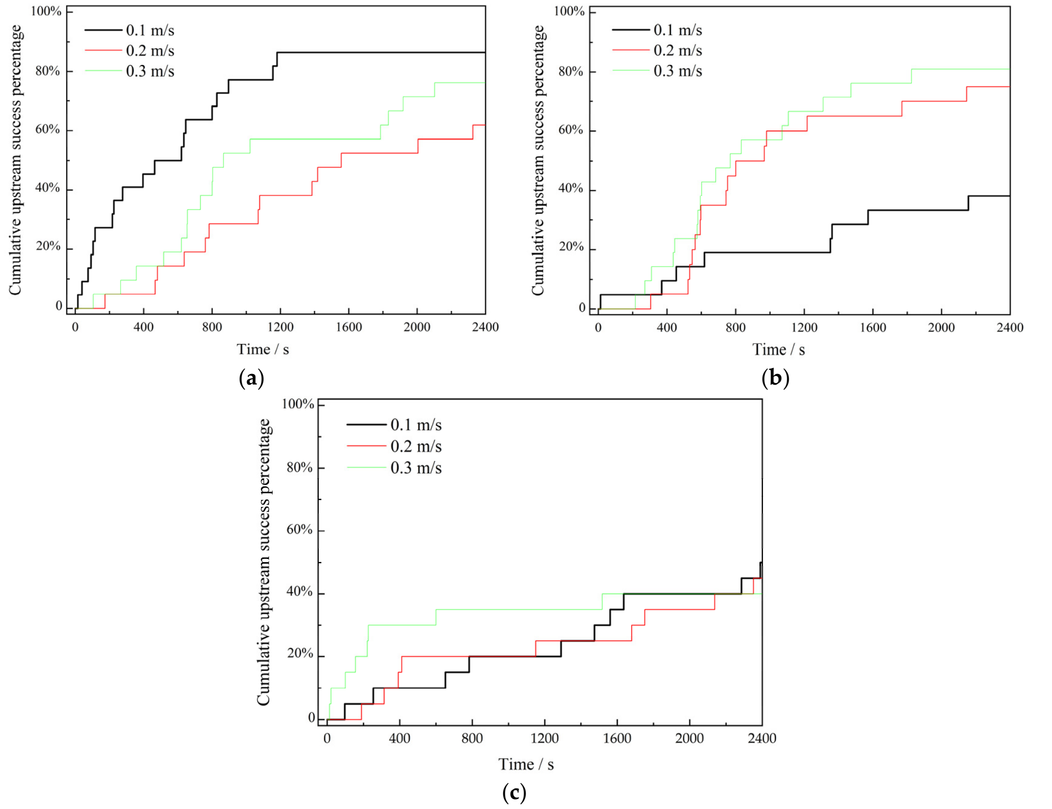

Figure 6. The cumulative passage efficiency of grass carp at (**a**) 30°, (**b**) 45°, and (**c**) 60° fishway entrance angles.

The average frequency of attracting fish to the fishway entrance at a 30° entrance angle was significantly higher than at 45° and 60° angles for grass carp. At a 30° entrance angle, the average frequency of attracting fish to the fishway entrance was 14.5 ± 2.48 times, 11.76 ± 2.11 times, and 13.41 ± 1.94 times when the velocity of the replenishment channel was 0.1 m/s, 0.2 m/s, and 0.3 m/s, respectively, at the entrance of the fishway (Figure 7a,b). At a 60° entrance angle, the average frequency of entering the fishway was 9.0 ± 2.36 times, 4.86 ± 1.77 times, and 4.54 ± 1.23 times when the velocity of the replenishment channel was 0.1 m/s, 0.2 m/s, and 0.3 m/s at the entrance of the fishway, respectively.

Interestingly, the distribution of grass carp was mainly in the zone between 1.4 and 4.4 m in the x direction and 2.05 and 2.46 m in the y direction. Thus, the fish movement behavior, including fish trajectories and residence times, was in this zone. The percentage of the residence time on the left bank at the entrance angles of 30° was significantly higher than at the entrance angles of 45° and 60°, as shown in Figure 8, and the tested fish mainly migrated from the left bank.

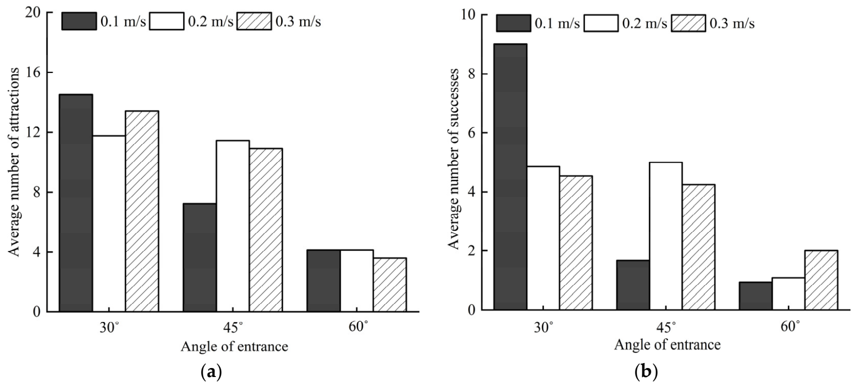

Figure 7. The average number of grass carp attracted to the fishway (**a**) and the average number of fish that entered into the fishway (**b**) at three different entrance angles and velocities of the replenishment channel.

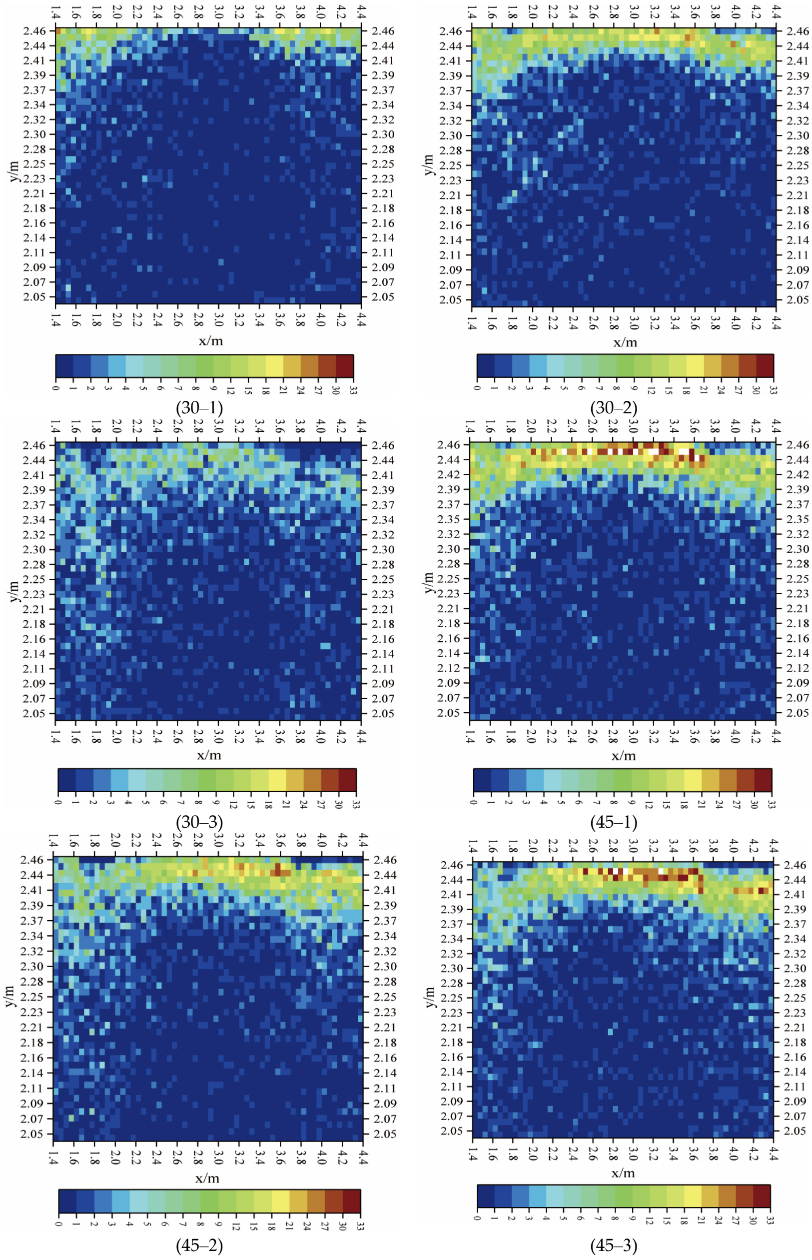

Figure 8. *Cont.*

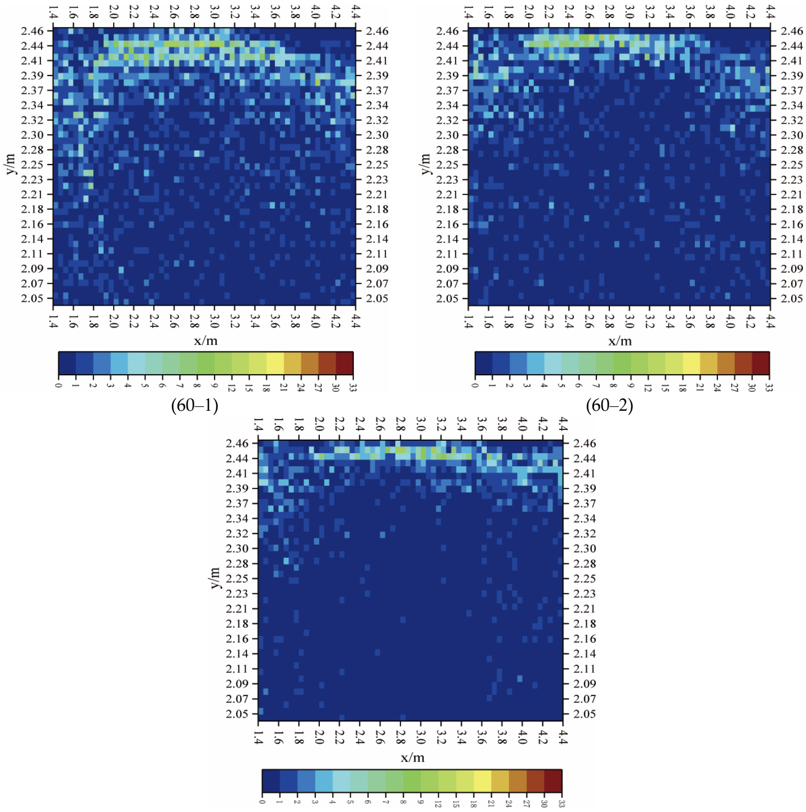

Figure 8. Heat map of movement trajectory for grass carp in the channel (note: 30–1, 30–2, 30–3, 45–1, 45–2, 45–3, 60–1, 60–2, and 60–3 represent the working conditions in Table 1).

3.3. Analysis of Energy Consumption

Approximately 93.01% (306/329) of grass carp could deflect and successfully enter the entrance with an entrance angle of 30°, and the frequency of fish head deflection was 329 times (Table 3). When the entrance angle was 45°, the frequency of fish head deflection was 229 times for grass carp, and a proportion of 82.97% (190/229) of grass carp deflected and entered the entrance. Grass carp deflected and entered the fishway entrance at a proportion of 54.66% (88/161) with an entrance angle of 60°. Among the three entrance angles, the results revealed that an entrance angle of 30° had a better entrance efficiency for the tested fish than entrance angles of 45° and 60° (Table 3).

Table 3. Frequency and efficiency of deflection of grass carp under nine working conditions.

Entrance Angle of Fishway	Working Conditions	The Number of Tested Fish (N^*)	The Frequency of Deflection for Fish in Each Working Condition (N)	Total Frequency of Deflection for Tested Fish (N^3)	Deflection Efficiency (N^4/N^3)
30°	30–1 30–2 30–3	22 21 21	148 90 91	329	93.01% (306/329)
45°	45–1 45–2 45–3	22 20 21	46 99 84	229	82.97% (190/229)
60°	60–1 60–2 60–3	20 20 20	57 53 51	161	54.66% (88/161)

Notes: N^* and N indicate the number of tested fish for each entrance angle and frequency of deflection in each working condition. N^3 and N^4 indicate the total frequency of deflection for tested fish in each entrance angle and the number of successful accesses in each entrance angle, respectively. The numbers 30–1, 30–2, 30–3, 45–1, 45–2, 45–3, 60–1, 60–2, and 60–3 represent the working conditions in Table 1.

According to the head deflection position of the fish and the distribution of water velocity, the water velocity was 0.32–0.50 m/s for grass carp when the fish head deflected into the entrance at an angle of 30°. The water velocity was 0.34–0.44 m/s for grass carp when the fish head deflected into the entrance at an angle of 45°, and the water velocity was 0.40–0.46 m/s when the fish head deflected into the entrance at an angle of 60°. Thus, the flow velocity was 0.32–0.50 m/s when the fish head deflected into the entrance under different entrance angles for grass carp (Figure 9).

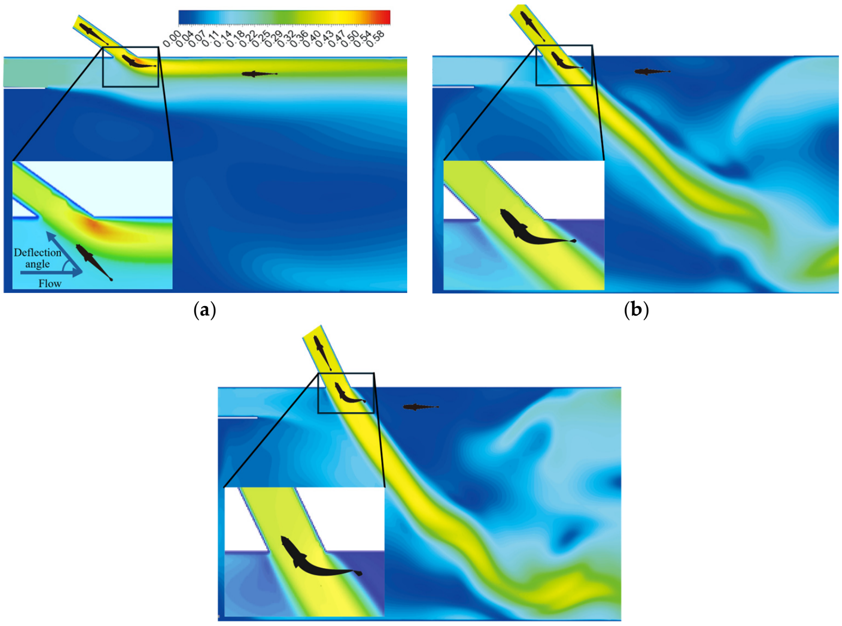

Figure 9. The deflection of fish head into the fishway at entrance angles of (**a**) 30°, (**b**) 45°, and (**c**) 60°.

The representative movement trajectories of the fish under different working conditions were used to analyze the energy consumption when grass carp entered the fishway entrance. As the entrance angle of the fishway increased, the fish's energy consumption increased, as shown in Figure 10. Additionally, there was a negative correlation between the entrance angle of the fishway and the deflection angle of the tested fish's head. The relative angle was formed by the direction of the fish body and the fishway entrance angle. For grass carp, the larger the deflection angle, the more energy that was consumed.

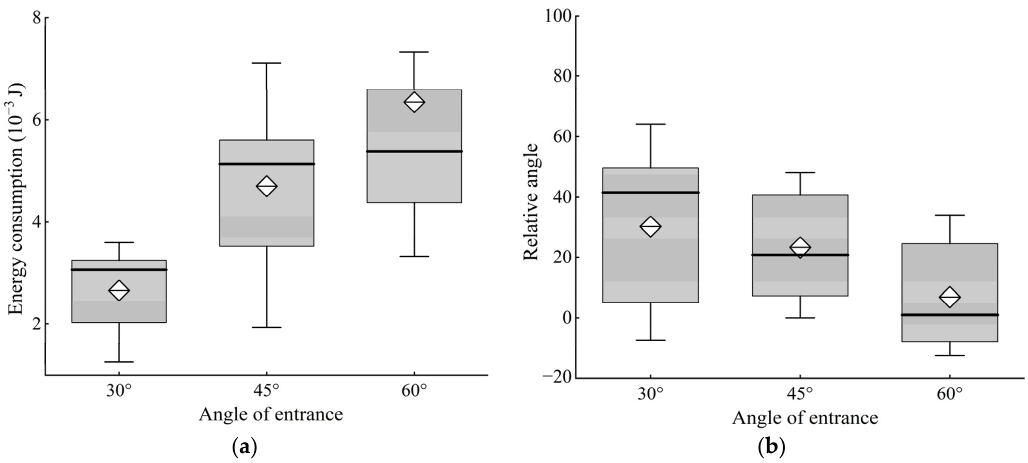

Figure 10. Box plots showing (**a**) the energy consumption and (**b**) the relative angle of entry into the fishway entrance for grass carp.

4. Discussion

4.1. Effects of Fishway Entrance Angle on Fishway Efficiency

In this study, hydraulics were analyzed at different entrance angles and replenishment flows. The entrance angle was altered and the direction of the water flow and flow pattern in the channel were varied. Three entrance angles formed three different distributions of water flow at the fishway entrance. The flow velocity is the key to attracting flow propagation [42,43]. The mainstream at the fishway entrance was mainly spread along the left bank at a 30° entrance angle, which made it easy for fish to quickly find the direction of the mainstream and then locate the entrance position [44,45]. When the fishway entrance angle was increased, the influencing scope of water was larger on the right bank, and the carp were more likely to be attracted by the flow on the right bank. Thus, the probability of entering the fishway entrance was reduced because it was not conducive to finding the fishway entrance along the right bank of the channel for carp. This might be why most of the fish moved along the left banks.

A suitable water velocity at the fishway entrance was important for attracting fish into the fishway [46–49]. When the water flow velocity was more than 0.21 m/s, grass carp were more likely to be attracted to the fishway entrance. If the flow velocity of the fishway entrance was too slow or too large, the fish could not detect the entrance [50–52]. In this study, the flow velocity was 0.32–0.50 m/s for grass carp when the fish head deflected into the entrance under different entrance angles. When the water velocity was more than 0.50 m/s, it caused disorientation and reduced the efficiency of the tested carps. Thus, a suitable fishway entrance angle and replenishment flow or velocity were the keys to attracting fish into the entrance. For migratory fish species, the location of the entrance and the distribution of the flow field are conducive to fish aggregations, which can improve the attraction efficiency of the entrance [53]. The study results regarding entrance angles were compared with the results regarding entrance arrangement obtained from previous research. The propriety of the location of the fishway was verified by using the numerical simulation and field investigation in previous research studies [54,55]. For example, the optimal location of fishway entrances seems to be in relatively low-velocity zones where fish aggregate at the tailrace channel exits. In this study, the entrance angle was changed, and the flow pattern of the entrance flow was altered accordingly. A relatively more effective entrance angle was found after the experiments. In future work, a greater number of different entrance angles and replenishment flows or velocity should be considered to find a more accurate relationship for entrance angles and replenishment flow or velocity for fishways.

4.2. Effects of Fishway Entrance Angle on Fish Movement Strategies

This study analyzed the relationship between fish movement behavior and entrance hydrodynamic conditions during migration [22,28,41,56,57]. When fish encounter water flow during migration, they have to resist the water flow and adjust their swimming movement posture to adapt to the changes in water flow, which cost energy [28,58–60]. When a fish moves in water, its head is the part of the body that changes the least, and the direction of the fish's head can indicate the direction of its body [61].

In this study, the representative trajectories of grass carps were chosen to obtain data on the behavior of the two species under different flow conditions, such as the frequency of fish head deflection, fish movement trajectories, transit time, deflection angle of the tested fish's head, attraction efficiency, cumulative entrance efficiency, and deflection efficiency. Combining the fish's swimming behavior and energy consumption, the relationship between the fish's deflection angle and energy consumption was analyzed. The results revealed that the deflection behavior of fish was related to different hydraulic factors of the fishway entrance [35,45,62]. Most of the tested fish swam along low-velocity zones and, thus, reduced their energy consumption during the process of migration. An entrance angle of 30° formed a mainstream that satisfied the velocity preferences for carp. When the entrance angle was different, the frequency of deflection and the deflection angle of the fish were significantly different. It is assumed that the mainstream direction is related to the preferred direction of fish, which affects the deflection behavior of fish [63]. Energy consumption and the deflection angle of the fish's head were analyzed for grass carp at different entrance angles. A large frequency of deflection and successful entrance efficiency and deflected efficiency were observed for grass carp when the fishway entrance angle was 30°. Compared with 45° and 60° entrance angles, the deflection angle of the fish's head decreased at a 30° entrance angle, resulting in lower energy consumption. The energy consumption and behavioral choices of fish in vertical slot fishways have been analyzed in previous studies by combining different flow patterns in fishways [26,59,64]. Previous studies have found that fish chose lower flow velocity and reduced energy expenditure paths when swimming through the fishway and proposed that by selecting smaller tail swinging angles and swinging frequency, the energy expenditure of fish during migration would be reduced [28,65]. It was further confirmed that a 30° entrance angle was the most suitable arrangement in this study.

When the flow velocity was high, energy consumption increased significantly, and the fish had to promptly adjust their posture to move into zones with more suitable water velocities [26,66], despite turbulence being another hydraulic factor that impacted fish movement [20,21]. More refined work on hydraulic parameters, such as turbulence [67–70]; shear stress [52,64,71–73]; and other movement behaviors, such as exercise fatigue [74–78], should be considered in future studies.

5. Conclusions

This study analyzed the swimming behavior of grass carp at a fishway entrance with different entrance angles (30°, 45°, and 60°) and replenishment flows. The results showed that a 30° entrance angle was better than 45° and 60° entrance angles under different working conditions, and the range of flow velocity was 0.32–0.50 m/s for grass carp when the fish head deflected into the entrance under different entrance angles. As the entrance angle of the fishway increased, the fish energy consumption increased. There was a negative correlation between the entrance angle of the fishway and the deflection angle of the tested fish's head. This research presents a reference that combines fish swimming behavior and hydraulics to optimize the design of fishway entrances.

Author Contributions: Y.M.: methodology, software, formal analysis, data curation, validation, visualization, writing—original draft preparation; J.T.: conceptualization, methodology, writing—review and editing, supervision, funding acquisition; H.T.: conceptualization, software, resources, data curation; J.S.: methodology, writing—review and editing; S.K.: supervision; M.L.: supervision; C.L.: supervision; X.S.: supervision, funding acquisition. All authors have read and agreed to the published version of the manuscript.

Funding: This research was funded by the National Natural Science Foundation of China (52179070, 52279069), the Innovative Research Group Program of the Natural Science Foundation of Hubei Province (2023AFA005), and Research Projects of China Three Gorges Construction (Group) Co., LTD. (JG/18056B, JG/18057B).

Data Availability Statement: The data that support the findings of this study are available from the corresponding author upon reasonable request.

Acknowledgments: The author would like to kindly thank Yuanyang Wang for his helpful suggestions.

Conflicts of Interest: The authors declare no conflicts of interest.

References

1. Cai, L.; Hou, Y.Q.; Katopodis, C.; He, D.; Johnson, D.; Zhang, P. Rheotaxis and swimming performance of Perch–barbel (*Percocypris pingi*, Tchang, 1930) and application to design of fishway entrances. *Ecol. Eng.* **2019**, *132*, 102–108. [CrossRef]
2. Kraabøl, M.; Museth, J. Efficiency of a fishway on brown trout (*Salmo trutta*) spawning populations. *Vann* **2019**, *4*, 295–311.
3. Song, C.; Omalley, A.; Roy, S.G.; Barber, B.L.; Zydlewski, J.; Mo, W. Managing dams for energy and fish tradeoffs: What does a win–win solution take? *Sci. Total Environ.* **2019**, *669*, 833–843. [CrossRef] [PubMed]

4. Li, G.N.; Sun, S.K.; Liu, H.T.; Zheng, T.G. *Schizothorax prenanti* swimming behavior in response to different flow patterns in vertical slot fishways with different slot positions. *Sci. Total Environ.* **2021**, *754*, 142142. [CrossRef] [PubMed]
5. Sanz–Ronda, F.J.; Fuentes–Pérez, J.F.; García–Vega, A.; Bravo–Córdoba, F.J. Fishways as downstream routes in small hydropower plants: Experiences with a Potamodromous Cyprinid. *Water* **2021**, *13*, 1041. [CrossRef]
6. Peterson, E.; Thors, R.; Frechette, D.; Zydlewski, J.D. Adult Sea Lamprey approach and passage at the Milford Dam fishway, Penobscot River, Maine, United States. *N. Am. J. Fish. Manag.* **2023**, *43*, 1052–1065. [CrossRef]
7. Rourke, M.L.; Robinson, W.; Baumgartner, L.J.; Doyle, J.; Growns, I.; Thiem, J.D. Sequential fishways reconnect a coastal river reflecting restored migratory pathways for an entire fish community. *Restor. Ecol.* **2018**, *27*, 399–407. [CrossRef]
8. Lothian, A.J.; Schwinn, M.; Anton, A.H.; Adams, C.E.; Newton, M.; Koed, A.; Lucas, M.C. Are we designing fishways for diversity? Potential selection on alternative phenotypes resulting from differential passage in brown trout. *J. Environ. Manag.* **2020**, *262*, 110317. [CrossRef]
9. Chen, M.; An, R.; Li, J.; Li, K.; Li, F. Identifying operation scenarios to optimize attraction flow near fishway entrances for endemic fishes on the Tibetan Plateau of China to match their swimming characteristics: A case study. *Sci. Total Environ.* **2019**, *693*, 133615. [CrossRef]
10. Liao, L.; Chen, M.; An, R.; Li, J.; Tang, X.; Yan, Z. Identifying three-dimensional swimming corridors for fish to match their swimming characteristics under different hydropower plant operations: Optimization of entrance location for fish-passing facilities. *Sci. Total Environ.* **2022**, *822*, 153599. [CrossRef]
11. Pedescoll, A.; Aguado, R.; Marcos, C.; González, G. Performance of a Pool and Weir Fishway for Iberian Cyprinids Migration: A Case Study. *Fishes* **2019**, *4*, 45. [CrossRef]
12. Bunt, C.M. Fishway entrance modifications enhance fish attraction. *Fish. Manag. Ecol.* **2001**, *8*, 95–105. [CrossRef]
13. Thiem, J.D.; Binder, T.R.; Dumont, P.; Hatin, D.; Hatry, C.; Katopodis, C.; Stamplecoskie, K.M.; Cooke, S.J. Multispecies fish passage behaviour in a vertical slot fishway on the Richelieu River, Quebec, Canada. *River Res. Appl.* **2012**, *29*, 582–592. [CrossRef]
14. Schütz, C.; Henning, M.; Czerny, R.; Herbst, M.; Pitsch, M. Addition of auxiliary discharge into a fishway—A contribution to fishway design at barrages of large rivers. *Ecol. Eng.* **2021**, *167*, 106257. [CrossRef]
15. Oufiero, C.E.; Whitlow, K.R. The evolution of phenotypic plasticity in fish swimming. *Curr. Zool.* **2016**, *62*, 475–488. [CrossRef] [PubMed]
16. Di Santo, V.; Goerig, E.; Wainwright, D.K.; Akanyeti, O.; Liao, J.C.; Castro–Santos, T.; Lauder, G.V. Convergence of undulatory swimming kinematics across a diversity of fishes. *Proc. Natl. Acad. Sci. USA* **2021**, *118*, e2113206118. [CrossRef] [PubMed]
17. Benitez, J.-P.; Dierckx, A.; Nzau Matondo, B.; Rollin, X.; Ovidio, M. Movement behaviours of potamodromous fish within a large anthropised river after the reestablishment of the longitudinal connectivity. *Fish. Res.* **2018**, *207*, 140–149. [CrossRef]
18. Tan, J.J.; Tan, H.L.; Goerig, E.; Ke, S.; Huang, H.Z.; Liu, Z.X.; Shi, X.T. Optimization of fishway attraction flow based on endemic fish swimming performance and hydraulics. *Ecol. Eng.* **2021**, *170*, 106332. [CrossRef]
19. Baumgartner, L.J.; Boys, C.; Marsden, T.; McPherson, J.; Ning, N.; Phonekhampheng, O.; Robinson, W.; Singhanouvong, D.; Stuart, I.G.; Thorncraft, G. A cone fishway facilitates lateral migrations of tropical River-Floodplain fish communities. *Water* **2020**, *12*, 513. [CrossRef]
20. Wang, X.; Wang, F.; Yang, J.N.; Yu, P. Modelling the hydraulic characteristics of diaphragm fishways and the effects on fish habitats. *Front. Environ. Sci.* **2022**, *10*, 977295. [CrossRef]
21. Sun, J.J.; Shi, J.Y.; Zhang, Q.; Shi, X.T.; Tan, J.J. Survey on performance of vertical slot and nature-like fishways at Angu hydropower station, Southwest China. *Water Sci. Eng.* **2024**, *17*, 83–91. [CrossRef]
22. Arenas, A.; Politano, M.; Weber, L.; Timko, M. Analysis of movements and behavior of smolts swimming in hydropower reservoirs. *Ecol. Model.* **2015**, *312*, 292–307. [CrossRef]
23. Haro, A.; Castro–Santos, T.; Noreika, J.; Odeh, M. Swimming performance of upstream migrant fishes in open-channel flow: A new approach to predicting passage through velocity barriers. *Can. J. Fish. Aquat. Sci.* **2004**, *61*, 1590–1601. [CrossRef]
24. Song, Y.Q.; Xie, S.G. Effects of substrate roughening on the swimming performance of *Schizothorax wangchiachii* (Fang, 1936) in the Heishui River: Implications for vertical slot fishway design. *J. Fish Biol.* **2023**, *104*, 473–483. [CrossRef] [PubMed]
25. Baek, K.O.; Lee, J.M.; Han, E.J.; Kim, Y.D. Evaluating attraction and passage efficiencies of pool-weir type fishways based on hydraulic analysis. *Appl. Sci.* **2022**, *12*, 1880. [CrossRef]
26. Tan, J.J.; Liu, Z.B.; Wang, Y.; Wang, Y.Y.; Ke, S.F.; Shi, X.T. Analysis of movements and behavior of bighead carps (*Hypophthalmichthys nobilis*) considering fish passage energetics in an experimental vertical slot fishway. *Animals* **2022**, *12*, 1725. [CrossRef]
27. Ye, Z.; Lian, X.; Bai, F.Q.; Hao, D.; Li, D.F.; Fang, Z.H. Response of upstream behavior and hydrodynamic factors of *Anguilla Japonica* in a combined bulkhead Fishway under tidal conditions. *Water* **2023**, *15*, 2585. [CrossRef]
28. Zhang, D.; Xu, Y.H.; Deng, J.; Shi, X.T.; Liu, Y.K. Relationships among the fish passage efficiency, fish swimming behavior, and hydraulic properties in a vertical-slot fishway. *Fish. Manag. Ecol.* **2024**, *31*, e12681. [CrossRef]
29. Cao, P.; Mu, X.P.; Li, X.; Baiyin, B.; Wang, X.Y.; Zhen, W.Y. Relationship between upstream swimming behaviors of juvenile grass carp and characteristic hydraulic conditions of a vertical slot fishway. *Water.* **2021**, *13*, 1299. [CrossRef]
30. Mu, X.P.; Cao, P.; Gong, L.; Baiyin, B.; Li, X.A. Classification method for fish swimming behaviors under incremental water velocity for fishway hydraulic design. *Water.* **2019**, *11*, 2131. [CrossRef]

31. Tan, J.J.; Li, H.; Guo, W.T.; Tan, H.L.; Ke, S.F.; Wang, J.B.; Shi, X.T. Swimming performance of four carps on the Yangtze River for fish passage design. *Sustainability* **2021**, *13*, 1575. [CrossRef]
32. Shi, X.T.; Ke, S.F.; Tu, Z.Y.; Wang, Y.M.; Tan, J.J.; Guo, W.T. Swimming capability of target fish from eight hydropower stations in China relative to fishway design. *Can. J. Fish. Aquat. Sci.* **2022**, *79*, 124–132. [CrossRef]
33. Yu, L.X.; Lin, J.Q.; Chen, D.Q.; Duan, X.B.; Peng, Q.D.; Liu, S.P. Ecological flow assessment to improve the spawning habitat for the four major species of carp of the Yangtze River: A study on habitat suitability based on ultrasonic telemetry. *Water* **2018**, *10*, 600. [CrossRef]
34. Duan, X.B.; Liu, S.P.; Huang, M.G.; Qiu, S.L.; Li, Z.H.; Wang, K.; Chen, D.Q. Changes in abundance of larvae of the four domestic Chinese carps in the middle reach of the Yangtze River, China, before and after closing of the Three Gorges Dam. *Environ. Biol. Fishes* **2009**, *86*, 13–22. [CrossRef]
35. Mu, X.P.; Zhen, W.Y.; Li, X.; Cao, P.; Gong, L.; Xu, F.R. A study of the impact of different flow velocities and light colors at the entrance of a fish collection system on the upstream swimming behavior of juvenile grass carp. *Water* **2019**, *11*, 322. [CrossRef]
36. Plew, D.R.; Klebert, P.; Rosten, T.W.; Aspaas, S.; Birkevold, J. Changes to flow and turbulence caused by different concentrations of fish in a circular tank. *J. Hydraul. Res.* **2015**, *53*, 364–383. [CrossRef]
37. Goodwin, R.A.; Politano, M.; Garvin, J.W.; Nestler, J.M.; Hay, D.; Anderson, J.J.; Weber, L.J.; Dimperio, E.; Smith, D.L.; Timko, M. Fish navigation of large dams emerges from their modulation of flow field experience. *Proc. Natl. Acad. Sci. USA* **2014**, *111*, 5277–5282. [CrossRef] [PubMed]
38. An, R.D.; Li, J.; Liang, R.F.; Tuo, Y.C. Three-dimensional simulation and experimental study for optimising a vertical slot fishway. *J. Hydro-Environ. Res.* **2016**, *12*, 119–129. [CrossRef]
39. Snyder, R.J. *Physiological Ecology of Pacific Salmon*; State University of New York College at Buffalo: Buffalo, NY, USA, 2011; Volume 125, pp. 819–820.
40. Vogel, S. *Life in Moving Fluids: The Physical Biology of Flow–Revised and Expanded Second Edition*; Princeton University Press: Princeton, NJ, USA, 2020.
41. Khan, L.A. A Three-Dimensional Computational Fluid Dynamics (CFD) Model analysis of free surface hydrodynamics and fish passage energetics in a vertical-slot fishway. *N. Am. J. Fish. Manag.* **2011**, *26*, 255–267. [CrossRef]
42. Heneka, P.; Zinkhahn, M.; Schütz, C.; Weichert, R.B. A parametric approach for determining fishway attraction flow at hydropower dams. *Water* **2021**, *13*, 743. [CrossRef]
43. Zeng, G.R.; Xu, M.S.; Mou, J.G.; Hua, C.C.; Fan, C.H. Application of Tesla Valve's obstruction characteristics to reverse fluid in fish migration. *Water* **2022**, *15*, 40. [CrossRef]
44. Zheng, T.G.; Niu, Z.P.; Sun, S.K.; Shi, J.Y.; Liu, H.T.; Li, G.N. Comparative study on the hydraulic characteristics of nature-like fishways. *Water* **2020**, *12*, 955. [CrossRef]
45. Farzadkhoo, M.; Kingsford, R.T.; Suthers, I.M.; Felder, S. Flow hydrodynamics drive effective fish attraction behaviour into slotted fishway entrances. *J. Hydrodyn.* **2023**, *35*, 782–802. [CrossRef]
46. Green, T.M.; Lindmark, E.M.; Lundström, T.S.; Gustavsson, L.H. Flow characterization of an attraction channel as entrance to fishways. *River Res. Appl.* **2011**, *27*, 1290–1297. [CrossRef]
47. Johnson, E.L.; Caudill, C.C.; Keefer, M.L.; Clabough, T.S.; Peery, C.A.; Jepson, M.A.; Moser, M.L. Movement of radio-tagged adult Pacific lampreys during a large-scale fishway velocity experiment. *Trans. Am. Fish. Soc.* **2012**, *141*, 571–579. [CrossRef]
48. Farzadkhoo, M.; Kingsford, R.T.; Suthers, I.M.; Geelan–Small, P.; Harris, J.H.; Peirson, W.; Felder, S. Attracting juvenile fish into Tube Fishways-roles of transfer chamber diameter and flow velocity. *Ecol. Eng.* **2022**, *176*, 106544. [CrossRef]
49. Liu, S.K.; Jian, Y.X.; Li, P.C.; Liang, R.F.; Chen, X.F.; Qin, Y.O.; Wang, Y.M.; Li, K.F. Optimization schemes to significantly improve the upstream migration of fish: A case study in the lower Yangtze River basin. *Ecol. Eng.* **2023**, *186*, 106838. [CrossRef]
50. Richer, E.E.; Fetherman, E.R.; Krone, E.A.; Wright, F.B.; Kondratieff, M.C. Multispecies fish passage evaluation at a rock-ramp fishway in a Colorado transition zone stream. *N. Am. J. Fish. Manag.* **2020**, *40*, 1510–1522. [CrossRef]
51. Baek, K.O.; Lee, J.M.; Ku, T.G.; Kim, Y.D. Evaluation of by-pass fishway operation for attraction efficiency based on GPS Drifter field experiments. *Water.* **2021**, *13*, 2302. [CrossRef]
52. Li, P.; Zhang, W.; Burnett, N.J.; Zhu, D.Z.; Casselman, M.; Hinch, S.G. Evaluating dam water release strategies for migrating adult Salmon using computational fluid dynamic modeling and biotelemetry. *Water Resour. Res.* **2021**, *57*, e2020WR028981. [CrossRef]
53. Yoon, J.-D.; Kim, J.-H.; Yoon, J.; Baek, S.-H.; Jang, M.-H. Efficiency of a modified Ice Harbor-type fishway for Korean freshwater fishes passing a weir in South Korea. *Aquat. Ecol.* **2015**, *49*, 417–429. [CrossRef]
54. Lindberg, D.-E.; Leonardsson, K.; Andersson, A.G.; Lundström, T.S.; Lundqvist, H. Methods for locating the proper position of a planned fishway entrance near a hydropower tailrace. *Limnologica* **2013**, *43*, 339–347. [CrossRef]
55. Baek, K.O.; Kim, Y.D. A case study for optimal position of fishway at low-head obstructions in tributaries of Han River in Korea. *Ecol. Eng.* **2014**, *64*, 222–230. [CrossRef]
56. Rodriguez, Á.; Bermúdez, M.; Rabuñal, J.R.; Puertas, J.; Dorado, J.; Pena, L.; Balairón, L. Optical fish trajectory measurement in fishways through computer vision and artificial neural networks. *J. Comput. Civ. Eng.* **2011**, *25*, 291–301. [CrossRef]
57. Elings, J.; Mawer, R.; Bruneel, S.; Pauwels, I.S.; Pickholtz, E.; Pickholtz, R.; Coeck, J.; Schneider, M.; Goethals, P. Linking fine-scale behaviour to the hydraulic environment shows behavioural responses in riverine fish. *Mov. Ecol.* **2023**, *11*, 50. [CrossRef]
58. Thiem, J.D.; Dawson, J.W.; Hatin, D.; Danylchuk, A.J.; Dumont, P.; Gleiss, A.C.; Wilson, R.P.; Cooke, S.J. Swimming activity and energetic costs of adult lake sturgeon during fishway passage. *J. Exp. Biol.* **2016**, *219*, 2534–2544. [CrossRef]

59. Kirk, M.A.; Caudill, C.C.; Syms, J.C.; Tonina, D. Context-dependent responses to turbulence for an anguilliform swimming fish, Pacific lamprey, during passage of an experimental vertical-slot weir. *Ecol. Eng.* **2017**, *106*, 296–307. [CrossRef]
60. Li, M.N.; An, R.D.; Chen, M.; Li, J. Evaluation of volitional swimming behavior of *Schizothorax prenanti* using an open-Channel flume with spatially heterogeneous turbulent flow. *Animals* **2022**, *12*, 752. [CrossRef]
61. Qian, Z.M.; Wang, S.H.; Cheng, X.E.; Chen, Y.Q. An effective and robust method for tracking multiple fish in video image based on fish head detection. *BMC Bioinform.* **2016**, *17*, 251. [CrossRef]
62. Tan, J.J.; Gao, Z.; Dai, H.C.; Yang, Z.Y.; Shi, X.T. Effects of turbulence and velocity on the movement behaviour of bighead carp (*Hypophthalmichthys nobilis*) in an experimental vertical slot fishway. *Ecol. Eng.* **2019**, *127*, 363–374. [CrossRef]
63. Chapman, J.W.; Klaassen, R.H.; Drake, V.A.; Fossette, S.; Hays, G.C.; Metcalfe, J.D.; Reynolds, A.M.; Reynolds, D.R.; Alerstam, T. Animal orientation strategies for movement in flows. *Curr. Biol.* **2011**, *21*, R861–R870. [CrossRef]
64. Gilja, G.; Ocvirk, E.; Fliszar, R. Experimental investigation of the Reynolds shear Stress exceedance rate for the injury and disorientation biocriteria boundary in the pool-orifice and vertical slot type fishways. *Appl. Sci.* **2021**, *11*, 7708. [CrossRef]
65. Xia, D.; Chen, W.S.; Liu, J.K.; Luo, X. The energy-saving advantages of burst-and-glide mode for thunniform swimming. *J. Hydrodyn.* **2018**, *30*, 1072–1082. [CrossRef]
66. Domenici, P.; Hale, M.E. Escape responses of fish: A review of the diversity in motor control, kinematics and behaviour. *J. Exp. Biol.* **2019**, *222*, jeb166009. [CrossRef]
67. Silva, A.T.; Santos, J.M.; Ferreira, M.T.; Pinheiro, A.N.; Katopodis, C. Effects of water velocity and turbulence on the behaviour of Iberian barbel (*Luciobarbus bocagei*, Steindachner 1864) in an experimental pool-type fishway. *River Res. Appl.* **2011**, *27*, 360–373. [CrossRef]
68. Tran, T.D.; Chorda, J.; Laurens, P.; Cassan, L. Modelling nature-like fishway flow around unsubmerged obstacles using a 2D shallow water model. *Environ. Fluid Mech.* **2015**, *16*, 413–428. [CrossRef]
69. Dizabadi, S.; Azimi, A.H. Hydraulic and turbulence structure of triangular labyrinth weir-pool fishways. *River Res. Appl.* **2019**, *36*, 280–295. [CrossRef]
70. Zheng, T.; Tu, C.; Sun, S.; Huang, W.; Ren, W.; Li, G.; Liu, H. Testing three vertical slot fishway configurations for a Chinese endemic fish. *J. Hydraul. Eng.* **2023**, *149*, 06023005. [CrossRef]
71. Quaresma, A.; Pinheiro, A. Modelling of pool–type fishways flows Efficiency and scale effects assessment. *Water* **2021**, *13*, 851. [CrossRef]
72. Cox, R.X.; Kingsford, R.T.; Suthers, I.; Felder, S. Fish injury from movements across hydraulic structures: A review. *Water.* **2023**, *15*, 1888. [CrossRef]
73. Zhang, D.; Bian, X.H.; Shi, X.T.; Deng, J.; Liu, Y.K. Design of a bilateral-symmetric multi-slot fishway and its comparison with vertical slot fishway in terms of hydraulic properties. *River Res. Appl.* **2023**, *39*, 954–969. [CrossRef]
74. Cai, L.; Chen, L.; Johnson, D.; Gao, Y.; Mandal, P.; Fang, M.; Tu, Z.Y.; Huang, Y.P. Integrating water flow, locomotor performance and respiration of Chinese sturgeon during multiple fatigue-recovery cycles. *PLoS ONE* **2014**, *9*, e94345. [CrossRef]
75. Laborde, A.; González, A.; Sanhueza, C.; Arriagada, P.; Wilkes, M.; Habit, E.; Link, O. Hydropower development, riverine connectivity, and non-sport fish species: Criteria for hydraulic design of fishways. *River Res. Appl.* **2016**, *32*, 1949–1957. [CrossRef]
76. Fuentes–Pérez, J.F.; García–Vega, A.; Sanz–Ronda, F.J.; Martínez de Azagra Paredes, A. Villemonte's approach: A general method for modeling uniform and non-uniform performance in stepped fishways. *Knowl. Manag. Aquat. Ecosyst.* **2017**, *418*, 23. [CrossRef]
77. Cai, L.; Zhang, P.; Johnson, D.; Zhao, P.; Hou, Y.Q.; Chen, X.J. Effects of prolonged and burst swimming on subsequent burst swimming performance of *Gymnocypris potanini firmispinatus* (Actinopterygii, Cyprinidae). *Hydrobiologia* **2019**, *843*, 201–209. [CrossRef]
78. Gisen, D.C.; Schutz, C.; Weichert, R.B. Development of behavioral rules for upstream orientation of fish in confined space. *PLoS ONE* **2022**, *17*, e0263964. [CrossRef]